C₆₀+C₆₀ molecular bonding revisited and expanded

Jorge Laranjeira, ^{1,*} Karol Strutyński, ² Leonel Marques, ¹ Emilio Martínez-Núñez, ³ and Manuel Melle-Franco^{2,†}

¹Departamento de Física and CICECO, Universidade de Aveiro, 3810-193 Aveiro, Portugal
²Departamento de Química and CICECO, Universidade de Aveiro, 3810-193 Aveiro, Portugal
³Departamento de Química Física, Universidade de Santiago de Compostela, 15782, Santiago de Compostela, Spain
(Dated: February 21, 2023)

Several dimerization products of fullerene C_{60} are presented and thoroughly characterized with a quantum chemical DFT model augmented by dispersion. We reanalyze and expand significantly the number of known dimers from 12 to 41. Many of the novel bonding schemes were found by analyzing more than 2 nanoseconds of high energy molecular dynamics semiempirical trajectories with AutoMeKin, a methodology previously used to compute the reactivity of much smaller molecules. For completeness, this was supplemented by structures built by different geometric considerations. Also, spin-polarization was explicitly considered yielding 12 new bonding schemes with magnetic ground states. The results are comprehensively analyzed and discussed in the context of yet to be explained 3D fullerene structures and recent fullerene 2D systems.

Keywords: Fullerene Dimers, DFT calculations, AutoMeKin, HOMO-LUMO Gap

INTRODUCTION

At room temperature and atmospheric pressure, C_{60} is a van der Waals solid with a face-centered cubic (fcc) structure where the molecules are rotating freely [1]. When subjected to visible or ultraviolet light, or high-pressures high-temperatures (HPHT) treatments the C_{60} molecules bond to each other via 66/66 2+2 cycloaddition forming aggregates and dimers [2–4], see figure 1.

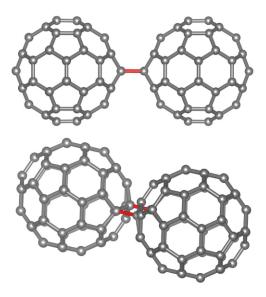


FIG. 1. Two views of the most stable and well studied C_{60} dimer with molecules bonded via 66/66~2+2 cycloaddition.

Increasing the pressure and temperature of the C_{60} HPHT treatment leads to the formation of extended

crystalline networks [5–11]. At pressures below 8 GPa the formation of low-dimensionality polymers occurs yielding 1D orthorhombic, 2D tetragonal and 2D rhombohedral phases. In all these low-dimensionality polymers, the molecules arrange themselves in covalently bonded chains (1D) or sheets (2D) formed exclusively by 66/66 2+2 cycloadditions.

It is above 8 GPa that fully 3D polymerized crystals are formed [8–11]. Here other bonding schemes, besides the 66/66 2+2 cycloaddition, start to play an important role, in fact, 3D polymers proposed to date have different bonding schemes such as the 56/56 2+2 cycloaddition [7, 8], the 6/6 3+3 cycloaddition and the double 66/66 4+4 cycloaddition [9], the 56/65 2+2 cycloaddition and the 5/5 3+3 cycloaddition [10] or even the double 5/5 2+3 cycloaddition [11].

Recently, other C_{60} polymers have been produced from a different route [12, 13]. This has yielded a pure carbon bulk material based on covalently linked fullerenes forming 2D sheets with hexagonal symmetry dubbed graphurelene [13]. These layers are bonded via single-bond and 56/65 2+2 cycloaddition, unlike any 2D polymers synthesized to date by HPHT treatment, showcasing the potential of alternative synthetic routes to produce new structures.

3D C_{60} polymers show quite remarkable physical properties for pure carbon phases, such as metallicity and low-compressibility which fosters interest in these materials [8–11]. Nevertheless, diffraction patterns from these phases lack the resolution needed to solve their crystalline structure. Thus, it is necessary to build complementary computational models fitting the overall symmetry and lattice parameters to the diffraction pattern and study their stability recurring to quantum simulation tools like Density Functional Theory (DFT) [7].

The distances between the two C_{60} covalently bonded molecules, i.e. a C_{60} dimer, computed from their molecular centers are similar to the corresponding

^{*} jorgelaranjeira@ua.pt

[†] manuelmelle@ua.pt

distance in a bulk crystalline phase. For instance, the C_{60} molecular distance, we compute for the 66/66 2+2 cycloaddition dimer, is ~ 9.1 Å while in the low-dimensionality polymers it is found to be between 9.02 and 9.18 Å [5, 6]. Also, for the recent graphulerene [12, 13], the computer dimer distances are 9.23 and 9.09 Å while the experimental bonding distance of 9.23 and 9.16 Å respectively. Hence, relating bonding distances to bonding schemes constitutes a simple yet accurate interpretation tool for the C_{60} crystal structure assignment, rendering covalent C_{60} dimers specifically relevant to compute and understand.

In the 90's and beginning of the 2000's, several studies regarding dimers were presented, nevertheless, to the best of our knowledge, no more than 12 dimers have been described altogether. Here, We consider, unless noted, C_{60} covalent dimers, that is dimers where the forming fullerene molecules are joined by intermolecular bonds. Strout et al. [4] performed probably the most extensive C_{60} dimerization study which addressed the 2+2 cycloadditions and a 2+4 cycloaddition. This last bonding scheme, following our notation, corresponds to a double 6/56 4+2 cycloaddition, since two 2+4 cycloaddition reactions, involving one hexagon (6) and one intramolecular single bond (56) each, are present.

Later, in 1994, Adams et al. [14] proposed three other bonding schemes, two bonding the molecules via their hexagons and one between their pentagons. the bonding between hexagons, the six atoms from one hexagon bond to the six atoms of the other hexagon, which can be obtained in the following two ways: 1) the hexagons of the two molecules align with each other (as well as the pentagons); 2) the hexagons from one molecule align with the pentagons of the other. When possible, we will keep the cycloaddition notation for the formed dimers nomenclature thus, in this case the dimers will be named, for instance, "triple 66/66 2+2 cycloaddition" (or "triple 56/56 2+2 cycloaddition") and "triple 56/66 2+2 cycloaddition" respectively. In the bonding between pentagons the five atoms from one pentagon bond to the five atoms of the other, the dimer will be referred to as "double 56/56 2+2 cycloaddition plus single bond". More details about this bonding nomenclature are available in the supporting information (SI) section A. In 2007 Liu et al. [15] studied again the two dimers bonded via hexagons confirming that they are thermodynamically stable and thus, could be observed experimentally.

Osawa et al. [16] reported the two possible 6/6 4+4 cycloaddition bonded dimers, while Matsuzawa et al. [17] also considered the 6/6 4+4 cycloaddition dimers and

added one of the two 66/6 2+4 cycloaddition dimers to their calculations. Besides the mentioned dimers, the single bond dimer (SB) was also considered [18]. In all of the works mentioned so far, the lowest energy dimer was consistently found to be the 66/66 2+2 cycloaddition [4, 14, 15, 18].

Apart from dimers formed just with pristine, i.e. unfunctionalized, C_{60} , there have also been numerous studies of dimers formed with other intermediates as well as coalescence products [4, 19, 20]. In addition, there have been studies on the dimerization and coalescence of C_{60} inside carbon nanotubes [5, 21, 22]. Note that although some of these systems also did appear in our calculations, for simplicity, they were not considered in our analysis and will not be discussed. Nevertheless, coalescence products might improve the understanding of amorphous carbon phase formation from C_{60} [23] or other phases were the C_{60} cage is broken [24] and might be the object of future studies.

The new systems reported here have been obtained fundamentally with AutoMeKin [25–27], an automatic computational procedure to find and characterize chemical reaction paths, and extended by manual construction following geometric considerations. report a total of 41 stable dimers computed at DFT level. From these, 25 were obtained with AutoMeKin, the others were built from geometric considerations or obtained from the literature. The molecular structure and relative stability of all dimers were computed at the TPSS-Def2-TZVPP/B3LYP-6-31G(d,p) theory level augmented by D3 dispersion with Becke-Johnson damping. All the dimers studied present C_{60} distances between 8.04 Å and 9.23 Å which renders some of these bridging patterns suitable candidates to be present in 3D C_{60} polymers.

METHODS

First, we performed a benchmark calculation of the dimer bonding energies for four different Hamiltonians, namely: TPSS-Def2-TZVPP-D3BJ/TPSS-6-31G(d,p)-D3BJ, TPSS-Def2-TZVPP-D3BJ/B3LYP-6-31G(d,p)-D3BJ, TPSS-6-31G(d,p)-D3BJ and B3LYP-6-31G(d,p)-D3BJ, on the lowest five energy C_{60} dimers, table I. The TPSS-Def2-TZVPP-D3BJ Hamiltonian was chosen after a recent benchmark study comparing the C_{60} isomerization energies with 115 methodologies which recommended this method based on its accuracy [28]. The bonding energy was computed by subtracting the energy of two isolated C_{60} to the energy of each dimer: $\Delta E_{Bond} = E_{dimer} - 2E_{C_{60}}$.

Theory level	Min1	Min2	Min3	Min4	Min5
B3LYP-6-31G(d,p)-D3BJ	-0.6541	0.2055	0.5839	1.0571	1.0934
	-0.5415				
TPSS-Def2-TZVPP-D3BJ/TPSS-6-31G(d,p)-D3BJ					
TPSS-Def2-TZVPP-D3BJ/B3LYP-6-31G(d,p)-D3BJ	-0.2494	0.4989	0.7440	1.2501	1.2771

TABLE I: Bonding energy of the five lowest energy $C_{60}+C_{60}$ dimers optimized with different levels of theory given in eV/dimer.

Theory level	ΔE_{Bond} (eV/dimer)	$\Delta E_{Bond} + BSSE (eV/dimer)$
B3LYP-6-31G(d,p)-D3BJ	-0.4569	-0.3512
TPSS-Def2-TZVPP-D3BJ/B3LYP-6-31G(d,p)-D3BJ	-0.3604	-0.3460

TABLE II: Bonding energy of the non-covalent $C_{60}+C_{60}$ dimer optimized with different levels of theory and corrected by the basis set superposition error (BSSE), given in eV/dimer.

The Basis Set Superposition Error (BSSE) was evaluated in a non-covalent dimer, and found to be sizable, around 0.1 eV, for bonding energies with the smaller, DZP, basis sets, table II. After the BSSE correction, both levels of theory yielded values differing less than 5 meV. Interestingly, relative energies were very similar, and also similar results were found for all DFT functionals. Considering this, we selected the TPSS-Def2-TZVPP-D3BJ/B3LYP-6-31G(d,p)-D3BJ methodology as it yields a good compromise between accuracy and computational cost. Namely, we performed the geometry optimizations at the B3LYP-6-31G(d,p) [29, 30] level augmented by the D3 van der Waals correction [31, 32] with Becke-Johnson damping [33] (B3LYP-6-31G(d,p)-D3BJ) followed by a single point calculation with TPSS-Def2-TZVPP Hamiltonian [34, 35] also augmented by the D3 van der Waals correction with Becke-Johnson damping (TPSS-Def2-TZVPP-D3BJ) for the energies. Hessian calculations were performed in all presented geometries at the B3LYP-6-31G(d,p)-D3BJ level to explicitly check the absence of negative frequencies. All calculations were performed with Gaussian 9 [36].

We explicitly analyzed the dispersion contribution to the bonding energy, as this contribution is missing in most early DFT and semiempirical studies. The dispersion correction shifts bonding energies to more binding values, for the B3LYP-6-31G(d,p) functional the maximum shift is 1.34 eV and the average one is 0.78 eV. For the TPSS-Def2-TZVPP functional the stabilization is lower, the maximum shift is 1.15 eV and the average 0.68 eV. This indicates that there is a consistent attractive dispersion contribution to the bonding interaction in all covalently bonded C_{60} dimers. In fact, without van der Waals correction, all dimers are metastable compared to the isolated C_{60} molecule, see SI table S1 and figures S1 and S2.

To systematically explore possible minima we employed AutoMeKin (AMK) [25–27], a software designed to find reaction mechanisms. AMK analyzes high-energy molecular dynamics trajectories via graph theory to search for structural transformations. When a structural transformation, such as bonds breaking or forming, is detected it finds and characterizes the transition state via its second-order derivatives. From the transition state, the intrinsic reaction coordinate (IRC) method is then used to obtain reactants and products. For this, 2.25 ns were run altogether via 4500, 500 fs long, independent molecular dynamics of two C_{60} molecules in a high energy bonding configuration. The dynamics were run with a specially modified version of MOPAC2016 [37] using the PM7 [38] Hamiltonian with a

time step of 0.5 fs. Note that AMK so far has been used in molecules ≤ 30 atoms [39], so this study, on a system with 120 atoms, showcases how the AMK methodology can be successfully extended to other problems.

In addition, for completeness, we have comprehensively searched for reported dimers in literature and also constructed other bonding schemes considering the geometric possibilities allowed by the molecule. the tables, the following labels reveal the procedure followed for each minimum: L, literature, G, geometric considerations and AMK. To build dimers from geometric considerations, we went through the possibilities of bonding between each molecular element of geometry avoiding large deformations. Three geometry elements: chemical bonds, pentagons, or hexagons were considered with a maximum of two of these elements being combined at a time. For instance, the two "5/6 3+3" bonds may be constructed taking into consideration the bridging of one pentagon to one hexagon while the "double 66/66 4+4" takes into consideration the bridging of two hexagons from each molecule. For simplicity, we only considered systems with an even number of intermolecular bonds in this procedure.

We present the HOMO-LUMO gaps at the B3LYP-6-31G(d,p) level as this Hamiltonian is expected to yield closer values to experiment [40]. Note that all calculations were first run without spin polarization, and, in the cases where structures were found to be unstable under these conditions, they were then run considering triplet or quintuplet ground states. This procedure yielded 12 dimers with spin-polarized ground states. In all cases, no initial symmetry constraints were used in the geometry optimizations.

RESULTS AND DISCUSSION

The dimer structures found are comprehensively summarized in table III by increasing energy with their symmetry, number of intermolecular bonds, HOMO-LUMO gap, bonding energy, the distance between C_{60} molecules and a label indicating the minima origin. A graphical rendering for all the bonding schemes found on these dimers together with some others that were found by AMK but are not stable at the DFT level, can be found on the SI, table S3. Relevantly, of the 12 dimers previously reported just the 6/66 2+4 cycloaddition reported by Matsuzawa et al. [17] was found not to be stable in our study, although it was found by AMK (AMK minimum 3097) indicating that at the semiempirical PM7 level, this dimer is stable.

Only one covalent dimer with a bonding energy of

-0.25 eV was found to be thermodynamically more stable, i.e. exothermic, than the isolated C_{60} molecules. In comparison, the less stable dimer is considerably more endothermic with a bonding energy of 7.95 eV. As a reference, we also computed the energy of the noncovalent dimer, -0.36 eV, which is more stable than the isolated molecule and any covalent dimer. These results match experimental observations since the only, experimentally observed, covalent dimer is fruit of the

66/66 2+2 cycloaddition [2–4] and at ambient conditions, C_{60} molecules are not covalently bound in the solid state. More exotic bonding configurations, for instance, corresponding to the 56/56 2+2 cycloaddition [8], can be found in three-dimensional crystals formed under high-pressure treatments, where the 66/66 2+2 cycloaddition bonding scheme alone cannot be used to bond all molecules in a three-dimensional extended system.

Minima	Dimer	Sym.	interm.	HOMO-LUMO	ΔE_{Bond}	Mol.	bond
order	name		bonds	gap (eV)	(eV/dimer)	dist. Å	origin
	C_{60}	I_{h}	0	2.8523	-	-	-
	Non covalent	C_1	0	2.59561	-0.3604	9.88	_
Min1	66/66 2+2	D_{2h}	2	2.50562	-0.2494	9.05	AMK66/L [4, 14, 16–18]
Min2	56/66 2+2	$C_{\rm s}$	2	1.81935	0.4989	9.07	AMK203/L [4]
Min3	SB	C_{2h}	1	1.9126*	0.7440	9.23	L [18]
Min4	56/65 2+2	C_{2h}	2	1.69636	1.2501	9.09	AMK1473/L [4]
Min5	56/56 2+2	C_{2v}	2	1.74996	1.2771	9.10	AMK1818/L [4]
Min6	double 66/66 2+2	C_{2v}	4	2.49311	1.4683	8.64	G ′ '
Min7	double $56/66\ 2+2\ M2$	$C_{\rm s}$	4	2.45719	1.8367	8.65	AMK1269
Min8	5/66 3+2	C_{s}	2	1.8779*	2.1629	8.91	AMK3333
Min9	double 56/56 2+2	C_{2v}	4	2.34045	2.2527	8.66	G
Min10	AMK5678	C_1	3	1.5557*	2.3363	8.85	AMK5678
Min11	6/66 3+2	C_1	2	0.74614	2.3867	8.87	AMK3615
Min12	6/6 4+4 M1	C_{2v}	2	1.97527	2.6221	8.81	AMK2506/L [16, 17]
Min13	triple 66/65 2+2	D_{3d}	6	2.39487	2.6419	8.44	L [14, 15]
Min14	6/6 4+4 M2	C_1	2	1.79731	2.6441	8.81	AMK2507/L [16, 17]
Min15	triple 66/66 2+2	D_{3h}	6	2.4327	2.6783	8.44	L [14, 15]
Min16	6/6 3+4 M2	C_1	2	1.8916*	2.8918	8.80	AMK4004
Min17	6/6 3+3 M3	C_2	2	1.8632*	3.1388	8.77	AMK5325
Min18	double 56/66 2+2 M1	$C_{\rm s}$	4	1.56792	3.2546	8.69	AMK2605
Min19	5/6 3+4 M2	$C_{\rm s}$	2	1.01063	3.3104	8.87	AMK4307
Min20	5/6 3+4 M1	$C_{\rm s}$	2	1.01798	3.3326	8.87	AMK4321
Min21	6/56 3+2 M2	C_1	2	1.6369*	3.3799	8.87	AMK4646
Min22	6/56 3+2 M1	C_1	2	1.6207*	3.4201	8.87	AMK4567
Min23	double 56/65 2+2	$C_{\rm s}$	$\overline{4}$	1.52057	3.6534	8.71	AMK3018
Min24	5/5 3+3 M1	C_{2h}	2	1.6465*	3.6760	8.89	G
Min25	6/6 3+4 M1	C_1	2	1.3896*	3.9138	8.77	AMK3893
Min26	double 56/56 2+2	C_{2v}	4	1.22506	4.4948	8.75	G
Min27	AMK6163	C_1	3	1.8342*	4.6261	8.41	AMK6163
Min28	double 56/56 2+2 plus SB	D_{5h}	5	0.74260	4.8285	8.68	L [14]
Min29	double 6/56 4+2	C_{2h}	4	2.34100	5.0253	8.62	L[4]
Min30	5/56 3+2 plus 6/56 4+2	$C_{\rm s}$	4	1.52955	5.1168	8.67	Ġ d
Min31	double 5/5 2+3	C_{2h}	4	1.10995	5.2631	8.72	G
Min32	5/6 3+3 plus 56/6 2+3	C_1	4	1.4211*	5.5353	8.62	AMK5775
Min33	AMK7077	$C_{\rm s}$	4	0.87974	6.3159	8.29	AMK7077
Min34	AMK6511	C_1	4	1.68194	6.4343	8.28	AMK6511
Min35	AMK7610	$C_{\rm s}$	4	0.95349	6.7170	8.25	AMK7610
Min36	5/5 3+3 plus 6/6 4+4	C_{2v}	4	0.76546	6.8452	8.05	G
Min37	double 56/65 3+4	C_{2h}	4	0.7584*	6.9087	8.10	G/AMK_or
Min38	5/6 3+4 plus 6/6 4+4	$C_{\rm s}$	4	0.94070	6.9973	8.04	G G
Min39	double 66/66 4+4	D_{2h}	4	1.64030	7.0261	8.05	Ĺ
Min40	AMK8161	$C_{\rm s}$	4	2.51216	7.5823	8.28	AMK8161
Min41	double 66/66 4+4	D_{2h}	6	2.01174	7.9499	8.16	G
	plus 66/66 2+2	211					_
E III. En	pergetics and distances of C	$c_0 + C$	co dimer	s computed at	' TPSS-Def2-T	ZVPP-1	D3B I/B3LVP-6-31G(d n)-

TABLE III: Energetics and distances of $C_{60}+C_{60}$ dimers computed at TPSS-Def2-TZVPP-D3BJ/B3LYP-6-31G(d,p)-D3BJ level. The HOMO-LUMO gaps presented were computed with B3LYP-6-31G(d,p)-D3BJ with * indicating that the presented value is an average of the α and β spin channels gaps (table S2 in SI has the used values). Letter L indicates a structure found in Literature while AMK and G indicate the structure was found using, respectively, AutoMeKin or geometric considerations. The number that follows AMK is an internal reference produced by AMK during the generation.

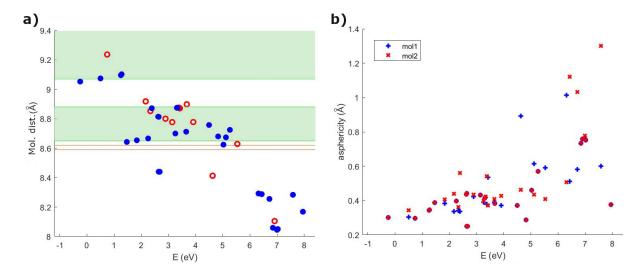


FIG. 2. a) Intermolecular distances as a function of the bonding energy computed at TPSS-Def2-TZVPP-D3BJ/B3LYP-6-31G(d,p)-D3BJ level of theory. Red circles indicate open-shell ground states and blue full circles closed-shell ground states. Red lines and green regions correspond to the experimental molecular distances reported by Yamanaka et al.[9] and Buga et al.[41] respectively. b) Asphericity as a function of the bonding energy. Blue cruxes and red x represent the two different C_{60} molecules in each dimer.

Relevantly, with more extreme pressures, higher energy minima can be reached with reduced C_{60} distances, fitting the trend shown in figure 2 a) where the distances between molecules show a monotonous decrease with increasing bonding energies. Furthermore, several of our dimers have shorter distances than reported coalescence products, see for instance the report by Strout et al. [4]. This indicates, that very short distances, below 8.3 Å, may alternatively be explained by C_{60} molecules bonded by the patterns reported here. Also, it is important to notice that although all the bonding schemes yield lower HOMO-LUMO gaps compared to C_{60} , no clear trend between this quantity and energy, number of bonds or intermolecular distance was found.

Interestingly, some of the found dimers are minima only with spin-polarized, triplet or quintuplet, wavefunctions. If the minimization is performed without spin-polarization, the dimers either break into C₆₀ molecules or transform into the more stable 66/66 2+2 cycloaddition dimer. Dimers with spin-polarized ground states, in table III, are marked with a star (*) in the HOMO-LUMO value. In addition, the value reported corresponds to the average gap for α and β electrons, all values are available on the SI, table S2. Minima 3, 8, 10, 27 and 37 have triplet ground states while minima 16, 17, 21, 22, 24, 25 and 32 have quintuplet ground states. This sheds light on the potential importance of spin-polarization in high-pressure polymerized C₆₀ since some of these bonds may be present in highpressure formed structures and thus, models built with them probably require spin-polarized Hamiltonians to be properly accounted for. In fact, Bernasconi et al. [42] took this into consideration while computing three-dimensional C_{60} polymers noticing that some of the modeled structures had more stable spin-polarized

ground states.

After the dimer formation, all the C_{60} molecules present some degree of deformation with respect to their original structure. To quantify the degree of molecular deformation we computed the asphericity of each molecule defined as the largest difference between the distance to the molecular center of mass for each atom and the same distance obtained for the pristine C_{60} , 3.51 Å. Asphericity values are summarized in table IV, relevantly, the dimers with higher symmetries than C_s have the same degree of deformation in both molecules, i.e. the same asphericity. In this case, asphericity values range from 0.25 Å for minima 13 and 15 to 0.75 Å for minima 37 and 39. Figure 2 b) shows the asphericity values as a function of the bonding energy. The asphericity qualitatively increases with increasingly endothermic bonding energies, indicating how higher deformation is clearly related to higher energetics and to the more extreme conditions needed for the synthesis of structures displaying these bonding schemes. In fact, the largest asphericity is found for one of the most energetic dimers, minimum 40, with a value of 1.30 Å.

AMK was crucial in finding exotic bonding schemes, like Minima 33 and 35 where one of the molecules is pinched allowing the bonding between one pentagon (for minimum 33 or hexagon for minimum 35) of one molecule to one hexagon and one pentagon of the other molecule, see figures 3 a) and b). This pinching implies a high asphericity value in the pinched molecule, ~ 1.0 Å, while the other molecule has nearly half that value in both dimers, see table IV. In both cases, this translates to remarkably short distances, ~ 8.25 Å, and is illustrative for dimers with short bonding distances, ≤ 8.4 Å. Furthermore, AMK found another peculiar bond, the double 5/5 2+3 cycloaddition (minimum 31), that was

Minima	asphericity	asphericity
	of molecule 1 (Å)	of molecule 2 (Å)
Min1	0.3018	0.3018
Min2	0.3034	0.3431
Min3	0.2977	0.2977
Min4	0.3439	0.3439
Min5	0.3470	0.3470
Min6	0.3889	0.3889
Min7	0.3831	0.4056
Min8	0.3376	0.4389
Min9	0.3980	0.3980
Min10	0.3406	0.3617
Min11	0.3365	0.5613
Min12	0.4364	0.4364
Min13	0.2504	0.2504
Min14	0.4421	0.4421
Min15	0.2513	0.2513
Min16	0.4239	0.4353
Min17	0.4334	0.4334
Min18	0.3909	0.3971
Min19	0.4140	0.4147
Min20	0.4191	0.4241
Min21	0.3786	0.5421
Min22	0.5351	0.3725
Min23	0.3899	0.4091
Min24	0.3826	0.3826
Min25	0.3717	0.4273
Min26	0.3726	0.3726
Min27	0.8917	0.4637
Min28	0.2869	0.2869
Min29	0.4599	0.4599
Min30	0.6149	0.4343
Min31	0.5692	0.5692
Min32	0.5916	0.4099
Min33	1.0139	0.5077
Min34	0.5109	1.1206
Min35	0.5816	1.0315
Min36	0.7341	0.7341
Min37	0.7595	0.7595
Min38	0.7623	0.7786
Min39	0.7520	0.7520
Min40	0.6009	1.3002
Min41	0.3764	0.3764

TABLE IV. Asphericities of each molecule in the $C_{60}+C_{60}$ dimers.

already present in a novel clathrate structure with very similar distances to the ones presented here [11].

Buga et al. [41] presented a series of six experimental crystalline phases obtained by pressurizing C_{60} between 11.5 and 13 GPa. In their report, structures are bodycentered orthorhombic with the Immm space group $(\Gamma_o^v D_{2h}^{25})$ in Schönflies notation) and presented their lattice parameters although no actual structure was proposed. Since their structures are body-centered orthorhombic, each of them has three distinct C_{60} distances, table V. In figure 2 a), we show a green area where these intermolecular distances lie. The longest distance found in this study is \sim 9.2 Å, in minimum 3. Note that as distances by different computational methods

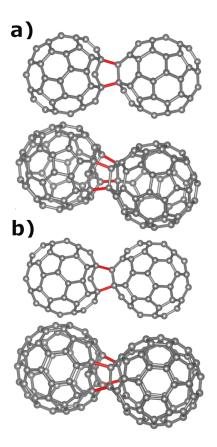


FIG. 3. Two distinct views of selected exotic bonding dimers found by AMK. a) Dimer AMK7077, min 33. b) Dimer AMK7610, min 35.

Sample $N^{\underline{o}}$	l		3	_	5	6
distance 1 (Å)						
distance 2 (Å)						
distance 3 (Å)	9.19	9.05	8.88	8.85	8.83	8.79

TABLE V. Intermolecular distances from the structures reported in [41].

may differ, if slightly, we have considered a ± 0.2 Å of length "flexibility" to our intermolecular distance values. In addition, molecules may also have additional deformations while in the crystalline phase, therefore hindering the direct correspondence between dimer distances and crystalline distances. This is observed, for instance, in the 66/66 2+2 cycloaddition dimer that shows different experimental distances lying between 9.02 and 9.18 Å [5, 6]. Hence, experimental intermolecular distances larger than 9.3 Å in table V, may be due to either a single bond or no bond between neighboring molecules. Interestingly, several experimental distances between 8.65 and 8.80 Å in table V are common distances in our dimers. Considering this, it seems likely that some of our bonding schemes are responsible for the distances found in these experimental phases.

In addition, there are other structures in the literature still to be resolved, like the one reported by Yamanaka et al. [9]. Although a complete crystalline structure was proposed, the structure changed considerably when optimized with DFT without constraints [42, 43]. Namely, Yamanaka et al. derived experimental lattice parameters of 7.86, 8.59 and 12.73 Å and a body-centered orthorhombic structure, with corresponding distances of 7.86, 8.59 and 8.62 Å, indicated in figure 2 a) by the red lines. The authors assigned these distances to double 66/66 4+4, no bond and 6/6 3+3 cycloaddition. respectively. Indeed, the 6/6 3+3 cycloaddition dimer, Min 17, and 66/664+4 cycloaddition dimer, min 39, have bonding distances in the appropriate range to explain this experimental data. Nevertheless, these bonding schemes were already used by Zipoli and Bernasconi [42] to construct crystalline structures and fail to reproduce the experimental lattice cell. Thus, other bonding schemes must be considered. We present here several potential alternatives within the observed range of distances.

Conversely, although the comparison of the distance is a simple, yet effective tool, we would like to emphasize that bonding patterns, which are stable in dimers may not be stable or not even geometrically possible in specific crystalline structures. For instance, minimum 4, although geometrically capable to bond to all the neighboring molecules in a crystalline fcc structure, turns out to be unstable in such configuration [7, 8]. On the other hand, the same minimum is present in other reported structures, such as in a 3D-rhombohedral phase [10] and in the recent graphullerene [13], proving that the molecular environment as a whole has to be considered to evaluate the existence of these patterns.

CONCLUSION

A comprehensive exploration and in-depth characterization of a large number of C_{60} dimers built from high energy molecular dynamics trajectories through the AMK methodology was performed. Several new C_{60} bonding schemes potentially relevant to understand polymeric phases were found and were energetically, structurally and electronically classified, increasing the number of known C_{60} dimers from 12 to 41. Some of the new dimers have bonding schemes matching experimental intermolecular distances observed on high-pressure high-temperature polymerized C_{60} yet to be understood, for instance in the works of Buga et al. or Yamanaka et al. [9, 41]. Relevantly,

12 of these dimers, i.e. 29 %, have spin-polarized ground states, which emphasizes that spin-polarization should be explicitly taken into consideration to properly model crystalline structures, especially with metallic or electronic exotic properties. This work paves the way for the exploration of novel extended 1D, 2D and 3D structures based on the bonding schemes presented here obtainable by HPHT treatment or more recent alternative routes [12, 13].

AUTHOR CONTRIBUTIONS

Conceptualization: M. Melle-Franco and J. Laranjeira; methodology: M. Melle-Franco, J. Laranjeira and E. Martínez-Núñez; software: M. Melle-Franco and E. Martínez-Núñez; validation: L. Marques, K. Strutyński and E. Martínez-Núñez; formal analysis: J. Laranjeira; investigation: J. Laranjeira; resources: M. Melle-Franco, E. Martínez-Núñez and J. Laranjeira; data curation: J. Laranjeira; writing-original draft preparation: J. Laranjeira; writing-review and editing: J. Laranjeira, M. Melle-Franco; visualization: J. Laranjeira; supervision: M. Melle-Franco; funding acquisition: M. Melle-Franco, E. Martínez-Núñez and J. Laranjeira. All authors have read and agreed to the published version of the manuscript.

ACKNOWLEDGMENTS

This work was developed within the scope of the project CICECO-Aveiro Institute of Materials, UIDB/50011/2020, UIDP/50011/2020 & $\rm LA/P/0006/2020,$ financed by national funds through the FCT/MCTES (PIDDAC) and IF/00894/2015 finances by FCT. J. Laranjeira acknowledges a PhD grant from FCT (SFRH/BD/139327/2018).

This work was partially supported by the Consellería de Cultura, Educación e Ordenación Universitaria (Grupo de referencia competitiva ED431C 2021/40), and the Ministerio de Ciencia e Innovación through Grant #PID2019-107307RB-I00.

The work has been performed under the project HPC-EUROPA3 (INFRAIA-2016-1-730897), with the support of the EC Research Innovation Action under the H2020 Programme; in particular, the author gratefully acknowledges the support of the computer resources and technical support provided by BSC.

^[1] A. Harris and R. Sachidanandam, Phys. Rev. B **46**, 4944 (1992).

^[2] A. Rao, P. Zhou, K.-A. Wang, G. Hager, J. Holden, Y. Wang, W.-T. Lee, X.-X. Bi, P. Eklund, D. Cornett, M. Duncan, and I. Amster, Science 259, 955 (1993).

^[3] V. Davydov, L. Kashevarova, A. Rakhmanina, V. Senyavin, O. Pronina, N. Oleynikov, V. Agafonov,

R. Céolin, H. Allouchi, and H. Szwarc, Chem. Phys. Lett. ${\bf 333},\,224\,$ (2001).

^[4] D. Strout, R. Murry, C. Xu, W. Eckhoff, G. Odom, and G. Scuseria, Chem. Phys. Lett. 214, 576 (1993).

^[5] M. Álvarez-Murga and J. Hodeau, Carbon 82, 381 (2015).

- [6] M. Núñez-Regueiro, L. Marques, J. L. Hodeau, O. Béthoux, and M. Perroux, Phys. Rev. Lett. 74, 278 (1995).
- [7] J. Laranjeira, L. Marques, M. Mezouar, M. Melle-Franco, and K. Strutyński, pss (RRL) 11, 1700343 (2017).
- [8] J. Laranjeira, L. Marques, N. Fortunato, M. Melle-Franco, K. Strutyński, and M. Barroso, Carbon 137, 511 (2018).
- [9] S. Yamanaka, A. Kubo, K. Inumaru, K. Komaguchi, N. S. Kini, T. Inoue, and T. Irifune, Phys. Rev. Lett. 96, 076602 (2006).
- [10] S. Yamanaka, N. S. Kini, A. Kubo, S. Jida, and H. Kuramoto, J. Am. Chem. Soc. 130, 4303 (2008).
- [11] J. Laranjeira, L. Marques, M. Melle-Franco, K. Strutyński, and M. Barroso, Carbon 194, 297 (2022).
- [12] L. Hou, X. Cui, B. Guan, S. Wang, R. Li, Y. Liu, D. Zhu, and J. Zheng, Nature 606, 507 (2022).
- [13] E. Meirzadeh, A. Evans, M. Rezaee, M. Milich, C. Dionne, T. Darlington, S. T. Bao, A. Bartholomew, T. Handa, D. Rizzo, R. Wiscons, M. Reza, A. Zangiabadi, N. Fardian-Melamed, A. Crowther, J. Schuck, D. Basov, X. Zhu, A. Giri, P. Hopkins, P. Kim, M. Steigerwald, J. Yang, C. Nuckolls, and X. Roy, Nature 613, 71 (2023).
- [14] G. Adams, J. Page, O. Sankey, and M. O'Keeffe, Phys. Rev. B 50, 17471 (1994).
- [15] F.-L. Liu and X.-X. Zhao, J. Mol. Struct.: THEOCHEM 804, 117 (2007).
- [16] S. Ōsawa, E. Ōsawa, and Y. Hirose, Fullerene sci. technol. 3, 565 (1995).
- [17] N. Matsuzawa, M. Ata, D. Dixon, and G. Fitzgerald, J. Phys. Chem. 98, 2555 (1994).
- [18] G. Scuseria, Chem. Phys. Lett. 257, 583 (1996).
- [19] P. Fowler, D. Mitchell, R. Taylor, and G. Seifert, J. Chem. Soc., Perkin Trans. 2, 1901 (1997).
- [20] M. Diudea, C. Nagy, O. Ursu, and T. Balaban, Fuller. Nanotub. Carbon Nanostructures 11, 245 (2003).
- [21] M. Koshino, Y. Niimi, E. Nakamura, H. Kataura, T. Okazaki, K. Suenaga, and S. Iijima, Nat. Chem. 2, 7 (2010).
- [22] T. Shimizu, D. Lungerich, K. Harano, and E. Nakamura, J. Am. Chem. Soc. 144, 9797 (2022).
- [23] S. Zhang, Z. Li, K. Luo, J. He, Y. Gao, A. Soldatov, V. Benavides, K. Shi, A. Nie, B. Zhang, W. Hu, M. Ma, Y. Liu, B. Wen, G. Gao, B. Liu, Y. Zhang, Y. Shu, D. Yu, X.-F. Zhou, Z. Zhao, B. Xu, L. Su, G. Yang, O. Chernogorova, and Y. Tian, Natl. Sci. Rev. 9, 10.1093/nsr/nwab140 (2021), nwab140.
- [24] F. Pan, K. Ni, T. Xu, H. Chen, Y. Wang, K. Gong, C. Liu, X. Li, M.-L. Lin, S. Li, X. Wang, W. Yan, W. Yin, P.-H. Tan, L. Sun, D. Yu, R. Ruoff, and Y. Zhu, Nature 614, 95 (2023).
- [25] E. Martínez-Núñez, J. Comput. Chem. 36, 222 (2015).
- [26] E. Martínez-Núñez, Phys. Chem. Chem. Phys. 17, 14912 (2015).

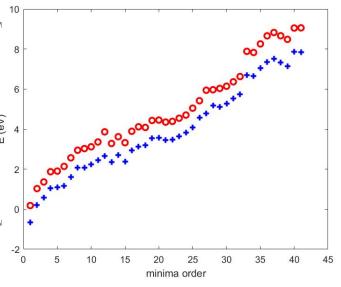
- [27] A. Rodríguez, R. Rodríguez-Fernández, S. Vázquez, G. Barnes, J. Stewart, and E. Martínez-Núñez, J. Comput. Chem. 39, 1922 (2018).
- [28] A. Karton, S. Waite, and A. Page, J. Phys. Chem. A 123, 257 (2019).
- [29] A. Becke, J. Chem. Phys. 98, 1372 (1993).
- [30] C. Lee, W. Yang, and R. Parr, Phys. Rev. B 37, 785 (1988).
- [31] S. Grimme, J. Antony, S. Ehrlich, and H. Krieg, J. Chem. Phys. 132, 154104 (2010).
- [32] S. Grimme, S. Ehrlich, and L. Goerigk, J. Comput. Chem. 32, 1456 (2011).
- [33] A. Becke and E. Johnson, J. Chem. Phys. 123, 154101 (2005).
- [34] J. Tao, J. Perdew, V. Staroverov, and G. Scuseria, Phys. Rev. Lett. 91, 146401 (2003).
- [35] F. Weigend and R. Ahlrichs, Phys. Chem. Chem. Phys. 7, 3297 (2005).
- [36] M. Frisch, G. Trucks, H. Schlegel, G. Scuseria, M. Robb, J. Cheeseman, G. Scalmani, V. Barone, G. Petersson, H. Nakatsuji, X. Li, M. Caricato, A. Marenich, J. Bloino, B. Janesko, R. Gomperts, B. Mennucci, H. Hratchian, J. Ortiz, A. Izmaylov, J. Sonnenberg, D. Williams-Young, F. Ding, F. Lipparini, F. Egidi, J. Goings, B. Peng, A. Petrone, T. Henderson, D. Ranasinghe, V. Zakrzewski, J. Gao, N. Rega, G. Zheng, W. Liang, M. Hada, M. Ehara, K. Toyota, R. Fukuda, J. Hasegawa, M. Ishida, T. Nakajima, Y. Honda, O. Kitao, H. Nakai, T. Vreven, K. Throssell, J. Montgomery, J. Peralta, F. Ogliaro, M. Bearpark, J. Heyd, E. Brothers, K. Kudin, V. Staroverov, T. Keith, R. Kobayashi, J. Normand, K. Raghavachari, A. Rendell, J. Burant, S. Iyengar, J. Tomasi, M. Cossi, J. M. Millam, M. Klene, C. Adamo. R. Cammi, J. Ochterski, R. Martin, K. Morokuma, O. Farkas, J. Foresman, , and D. Fox, Gaussian 09 revision A.02, gaussian Inc. Wallingford CT, 2016.
- [37] J. Stewart, Computational chemistry: Colorado springs, co., http://openmopac.net (2016). [accessed on 31/01/2023].
- [38] J. Stewart, J. Mol. Model. 19, 1 (2013).
- [39] R. Jara-Toro, G. Pino, D. Glowacki, R. Shannon, and E. Martínez-Núñez, ChemSystemsChem 2, e1900024 (2020)
- [40] K. Sohlberg and M. Foster, RSC Adv. 10, 36887 (2020).
- [41] S. Buga, V. Blank, N. Serebryanaya, A. Dzwilewski, T. Makarova, and B. Sundqvist, Diam. Relat. Mater. 14, 896 (2005).
- [42] F. Zipoli and M. Bernasconi, Phys. Rev. B 77, 115432 (2008).
- [43] J. Yang, J. Tse, and T. Iitaka, J. Chem. Phys. 127, 134906 (2007).

SUPPORTING INFORMATION

A. BONDING NOTATION

The naming of $C_{60}+C_{60}$ bonding schemes is done following the so-called cycloaddition rules which state how different rings react in organic chemistry in order to fuse. Considering the formation of a new ring of bonds between two molecules the bonding scheme is classified by the geometrical figure (or combination of geometrical figures) that is facing each molecule and by the number of atoms from each molecule that is involved in it. If we consider the more common, and stable, C_{60} dimer, the intermolecular bonding follows a 66/66 2+2 cycloaddition: 2+2 because from each molecule there are two bonds involved (one intramolecular and one intermolecular), and 66/66 since the two carbon atoms from each molecule are covalently bonded to the other by the two carbon atoms shared by two hexagons (hence 66 for each molecule). We may also consider that the alignment is done just by one geometrical figure from each molecule. If we consider the alignment between two hexagons, we will have a 6/6 n+m cycloaddition. With n, and m being integers smaller than 4.

B. VAN DER WAALS CORRECTION AND EXCHANGE-CORRELATION COMPARISON



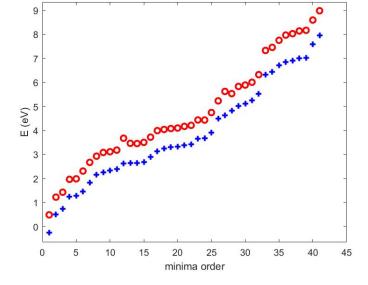


Figure S1. Minima bonding energy in eV per dimer vs minima order computed with B3LYP-6-31G(d,p) Hamiltonian (red circles) and augmented by the D3 van der Waals correction with finite Becke–Johnson damping (blue cruxes) after optimization at B3LYP-6-31G(d,p)-D3BJ level.

Figure S 2. Minima bonding energy in eV per dimer vs minima order computed with TPSS-Def2-TZVPP Hamiltonian (red circles) and augmented by the D3 van der Waals correction with finite Becke–Johnson damping (blue cruxes) after optimization at B3LYP-6-31G(d,p)-D3BJ level.

Minima	Dimer	Sym	interm.	$\mathbb{E}_{Bond}^{B3LYP}$	$\mathbf{E}_{Bond}^{B3LYP-D3BJ}$	$\left \mathbf{E}_{Bond}^{TPSS-D3BJ} \right $	\mathbb{E}_{Bond}^{TPSS}
order	name	Sy 1111.	bonds	(eV/dim)	(eV/dim)	(eV/dim)	(eV/dim)
Min1	66/66 2+2	D_{2h}	2	0.1823	-0.6541	-0.2494	0.4900
Min2	56/66 2+2	$C_{\rm s}$	2	1.0300	0.2055	0.4989	1.2269
Min3	SB	C_{2h}	1	1.3613	0.5839	0.7440	1.4314
Min4	56/65 2+2	C_{2h}	2	1.8711	1.0571	1.2501	1.9679
Min5	56/56 2+2	C_{2v}	2	1.9026	1.0934	1.2771	1.9906
Min6	double 66/66 2+2	C_{2v}	$\frac{1}{4}$	2.1376	1.1710	1.4683	2.3126
Min7	double $56/66 \ 2+2 \ M2$	$C_{\rm s}$	4	2.5666	1.6022	1.8367	2.6752
Min8	5/66 3+2	$C_{\rm s}$	2	2.9455	2.0740	2.1629	2.9319
Min9	double 56/56 2+2	C_{2v}	$\frac{1}{4}$	3.0279	2.0741	2.2527	3.0859
Min10	AMK5678	C_1	3	3.1171	2.2272	2.3363	3.1170
Min11	6/66 3+2	C_1	2	3.3582	2.4498	2.3867	3.1851
Min12	6/6 4+4 M1	C_{2v}	2	3.8631	2.6621	2.6221	3.6790
Min13	triple 66/65 2+2	D_{3d}	6	3.2816	2.3517	2.6419	3.4678
Min14	6/6 4+4 M2	C_1	2	3.6203	2.6950	2.6441	3.4582
Min15	triple 66/66 2+2	D_{3h}	6	3.3219	2.3890	2.6783	3.5086
Min16	6/6 3+4 M2	C_1	2	3.8909	2.9370	2.8918	3.7243
Min17	6/6 3+3 M3	C_2	2	4.1152	3.1303	3.1388	3.9958
Min18	double 56/66 2+2 M1	$C_{\rm s}$	4	4.0830	3.1872	3.2546	4.0437
Min19	5/6~3+4~M2	$C_{\rm s}$	2	4.4326	3.5528	3.3104	4.0827
Min20	5/6 3+4 M1	$C_{\rm s}$	2	4.4504	3.5723	3.3326	4.1037
Min21	6/56 3+2 M2	C_1	2	4.3499	3.4470	3.3799	4.1725
Min22	6/56 3+2 M1	C_1	2	4.3866	3.4796	3.4201	4.2159
Min23	double $56/65\ 2+2$	$C_{\rm s}$	4	4.5444	3.6441	3.6534	4.4392
Min24	5/5 3+3 M1	C_{2h}	2	4.7005	3.8357	3.6760	4.4361
Min25	6/6 3+4 M1	C_1	2	5.0466	4.0917	3.9138	4.7480
Min26	double $56/56\ 2+2$	C_{2v}	4	5.4181	4.5818	4.4948	5.2343
Min27	AMK6163	C_1	3	5.9410	4.7803	4.6261	5.6268
Min28	double $56/56$ $2+2$ plus SB	D_{5h}	5	5.9654	5.1727	4.8285	5.5361
Min29	double $6/56\ 4+2$	C_{2h}	4	6.0320	5.1107	5.0253	5.8338
Min30	5/56 3+2 plus 6/56 4+2	$C_{\rm s}$	4	6.1424	5.2653	5.1168	5.8918
Min31	double $5/5\ 2+3$	C_{2h}	4	6.3630	5.5234	5.2631	6.0079
Min32	5/6 3+3 plus 56/6 2+3	C_1	4	6.6255	5.7290	5.5353	6.3257
Min33	AMK7077	$C_{\rm s}$	4	7.8846	6.7070	6.3159	7.3327
Min34	AMK6511	C_1	4	7.8269	6.6398	6.4343	7.4601
Min35	AMK7610	$C_{\rm s}$	4	8.2559	7.0520	6.7170	7.7550
Min36	5/5 3+3 plus 6/6 4+4	C_{2v}	4	8.6573	7.3448	6.8452	7.9718
Min37	double $56/65 \ 3+4$	C_{2h}	4	8.8244	7.5147	6.9087	8.0303
Min38	5/6 3+4 plus 6/6 4+4	$C_{\rm s}$	4	8.6623	7.3213	6.9973	8.1441
Min39	double 66/66 4+4	D_{2h}	4	8.4821	7.1399	7.0261	8.1709
Min40	AMK8161	$C_{\rm s}$	4	9.0487	7.8726	7.5823	8.5970
Min41	double 66/66 4+4	D_{2h}	6	9.0574	7.8481	7.9499	8.9845
	plus 66/66 2+2						, ,,,,

Table S1. Bonding energy of $C_{60}+C_{60}$ dimers optimized with B3LYP-6-31G(d,p) augmented with D3 van der Waals correction with finite Becke–Johnson damping and computed with B3LYP-6-31G(d,p) and TPSS-Def2-TZVPP/B3LYP-6-31G(d,p)-D3BJ, with and without D3 van der Waals correction with finite Becke–Johnson damping augmentation.

C. COMPLETE HOMO-LUMO GAP INFORMATION

Minima	Dimer	Sym.	interm.	HOMO-LUMO	ΔE_{Bond}	Mol.
order	name		bonds	gap (eV)	(eV/dim)	dist. Å
	C_{60}	$I_{\rm h}$	0	2.8523	-	
Min1	66/66 2+2	D_{2h}	2	2.50562	-0.6541	9.05
Min2	56/66 2+2	$C_{\rm s}$	2	1.81935	0.2055	9.07
Min3	SB	C_{2h}	1	1.84359 1.98155	0.5839	9.23
Min4	56/65 2+2	C_{2h}	2	1.69636	1.0571	9.09
Min5	56/56 2+2	C_{2v}	2	1.74996	1.0934	9.10
Min6	double $66/66\ 2+2$	C_{2v}	4	2.49311	1.1710	8.64
Min7	double $56/66\ 2+2\ M2$	$C_{\rm s}$	4	2.45719	1.6022	8.65
Min8	5/66 3+2	$C_{\rm s}$	2	1.91651 1.83923	2.0740	8.91
Min9	double $56/56\ 2+2$	C_{2v}	4	2.34045	2.0741	8.66
Min10	AMK5678	C_1	3	1.41609 1.69528	2.2272	8.85
Min11	6/66 3+2	C_1	2	0.74614	2.4498	8.87
Min12	6/6 4+4 M1	C_{2v}	2	1.97527	2.6621	8.81
Min13	triple $66/65\ 2+2$	D_{3d}	6	2.39487	2.3517	8.44
Min14	6/6 4+4 M2	C_1	2	1.79731	2.6950	8.81
Min15	triple 66/66 2+2	D_{3h}	6	2.4327	2.3890	8.44
Min16	$6/6 \; 3+4 \; M2$	C_1	2	1.78589 1.99733	2.9370	8.80
Min17	6/6 3+3 M3	C_2	2	1.78318 1.94318	3.1303	8.77
Min18	double $56/66 \ 2+2 \ M1$	$C_{\rm s}$	4	1.56792	3.1872	8.69
Min19	5/6 3+4 M2	$C_{\rm s}$	2	1.01063	3.5528	8.87
Min20	5/6 3+4 M1	$C_{\rm s}$	2	1.01798	3.5723	8.87
Min21	6/56 3+2 M2	C_1	2	1.53201 1.74182	3.4470	8.87
Min22	6/56 3+2 M1	C_1	2	1.51841 1.72304	3.4796	8.87
Min23	double $56/65\ 2+2$	$C_{\rm s}$	4	1.52057	3.6441	8.71
Min24	5/5 3+3 M1	C_{2h}	2	1.8637 1.4294	3.8357	8.89
Min25	6/6 3+4 M1	C_1	2	1.28058 1.49854	4.0917	8.77
Min26	double $56/56\ 2+2$	C_{2v}	4	1.22506	4.5818	8.75
Min27	AMK6163	C_1	3	1.75270 1.91569	4.7803	8.41
Min28	double $56/56$ 2+2 plus SB	D_{5h}	5	0.74260	5.1727	8.68
Min29	double $6/56\ 4+2$	C_{2h}	4	2.34100	5.1107	8.62
Min30	5/56 3+2 plus 6/56 4+2	$C_{\rm s}$	4	1.52955	5.2653	8.67
Min31	double $5/5\ 2+3$	C_{2h}	4	1.10995	5.5234	8.72
Min32	5/6 3+3 plus 56/6 2+3	C_1	4	1.39868 1.44358	5.7290	8.62
Min33	AMK7077	$C_{\rm s}$	4	0.87974	6.7070	8.29
Min34	AMK6511	C_1	4	1.68194	6.6398	8.28
Min35	AMK7610	$C_{\rm s}$	4	0.95349	7.0520	8.25
Min36	5/5 3+3 plus 6/6 4+4	C_{2v}	4	0.76546	7.3448	8.05
Min37	double $56/65 \ 3+4$	C_{2h}	4	0.85662 0.66015	7.5147	8.10
Min38	5/6 3+4 plus 6/6 4+4	$C_{\rm s}$	4	0.94070	7.3213	8.04
Min39	double 66/66 4+4	D_{2h}	4	1.64030	7.1399	8.05
Min40	AMK8161	$C_{\rm s}$	4	2.51216	7.8726	8.28
Min41	double $66/66 \ 4+4$	D_{2h}	6	2.01174	7.8481	8.16
	plus 66/66 2+2					

Table S2. Energetics and molecular distances of $C_{60}+C_{60}$ dimers computed at B3LYP-6-31G(d,p)-D3BJ level of theory. Letter L indicate structure found in Literature, AMK and G indicate the structure was found using, respectively, AutoMeKin or geometric considerations. The number that follows AMK is simple the energy order of the minimum given by AMK.

D. BONDING SCHEMES

Table S3. $C_{60}+C_{60}$ dimer names, number of bonds, bonding schemes and origin of the bond. Letter L indicate structure found in Literature, AMK and G indicate that the structure was found using, respectively, AutoMeKin or geometric considerations. The number that follows AMK is simple the energy order of the minimum given by AMK.

Isomer	interm. bonds	intermolecular bonding scheme	bond origin
C_{60}	0	-	-
Min1 66/66 2+2	2		AMK66/L [1–5]
Min2 56/66 2+2	2		AMK203/L [1]
Min3 single bond	1		L [3]
Min4 56/65 2+2	2		AMK1473/L [1]
Min5 56/56 2+2	2		AMK1818/L [1]

Min6 double 66/66 2+2	4	G
Min7 double 56/66 2+2 M2	4	AMK1269
Min8 5/66 3+2	2	AMK3333
Min9 double 56/56 2+2	4	G
Min10 AMK5678	3	AMK5678
Min11 6/66 3+2	2	AMK3615

Min 12 6/6 4+4 M1	2	AMK2506/L [4,
Min13 triple 66/65 2+2	6	AMK1372/L [2
Min 14 6/6 4+4 M2	2	AMK2507/L [4
Min15 triple 66/66 2+2	6	L [2, 6]
Min 16 6/6 3+4 M2	2	AMK4004
Min 17 6/6 3+3 M3	2	AMK5325

Min18 double 56/66 2+2 M1	4	AMK2605
Min 19 5/6 3+4 M2	2	AMK4307
Min 20 5/6 3+4 M1	2	AMK4321
Min 21 6/56 3+2 M2	2	AMK4646
Min22 6/56 3+2 M1	2	AMK4567
Min23 double 56/65 2+2	4	AMK3018

Min 24 5/5 3+3 M1	2	G
Min25 6/6 3+4 M1	2	AMK3893
Min 26 double 56/56 2+2	4	G
Min 27 AMK6163	3	AMK6163
Min 28 double 56/56 2+2 plus	SB 5	L [2]
Min 29 double 6/56 4+2	4	L [1]
Min 30 5/56 3+2 plus		G
6/56 4+2	4	

Min 31 double 5/5 2+3	4	G
Min 32 5/6 3+3 plus 56/6 2+3	4	AMK577
Min 33 AMK7077	4	AMK707
Min 34 AMK6511	4	AMK651
Min35 AMK7610	4	AMK761
Min36 5/5 3+3 plus 6/6 4+4	4	G

Min37 double 56/65 3+4	4	S-AMK_or
Min38 5/6 3+4 plus 6/6 4+4	4	G
Min39 double 66/66 4+4	4	G
Min 40 AMK8161	4	AMK8161
Min41 double 66/66 4+4 plus	6	G
plus 66/66 2+2 double 66/6 2+4	4	G

66/6 2+4	2		AMK3097/L [5]
5/5 3+3 M2	2	()	G
5/56 3+2	2		G
5/65 3+2	2		G
6/6 3+3 M1	2		G
6/6 3+3 M2	2		AMK5282
6/6 3+3 M4	2		G

6/56 4+2 M1 2	G
6/56 4+2 M2 2	G
6/56 4+2 plus 6/66 4+2 4	G
5/66 3+2 plus 6/56 4+2 4	G
5/6 3+3 M1 2	AMK5118
double 66/66 4+4 zig 4	G
double 56/65 3+4 zig 4	G

5/5 3+3 plus 6/6 4+4 zig	4	G
double 66/66 4+4 plus double 56/56 2+2	4	G
AMK5282	3	
AMK6480	4	AMK6480

^[1] D. Strout, R. Murry, C. Xu, W. Eckhoff, G. Odom, and G. Scuseria, Chem. Phys. Lett. 214, 576 (1993).

^[2] G. Adams, J. Page, O. Sankey, and M. O'Keeffe, Phys. Rev. B **50**, 17471 (1994).

^[3] G. Scuseria, Chem. Phys. Lett. **257**, 583 (1996).

^[4] S. Ōsawa, E. Ōsawa, and Y. Hirose, Fullerene sci. technol. 3, 565 (1995).

^[5] N. Matsuzawa, M. Ata, D. Dixon, and G. Fitzgerald, J. Phys. Chem. 98, 2555 (1994).

^[6] F.-L. Liu and X.-X. Zhao, J. Mol. Struct.: THEOCHEM 804, 117 (2007).